PERMEABILITY MEASUREMENTS ON HYDRATE-BEARING SANDSTONE CORES WITH EXCESS WATER

Stian Almenningen, Håkon Juliussen and Geir Ersland
Department of Physics and Technology, University of Bergen

ABSTRACT
Methane hydrates exist in large quantities in natural sediments and methane gas can be produced from them by either dissociating the hydrate structure or by injecting a more stable hydrate former, which leads to spontaneous exchange of guest molecules. In either way, it is important with sufficient permeability to allow for injection and extraction of fluids. The effect of hydrate saturation on effective gas permeability is reported in this paper. Bentheim sandstone cores with high intrinsic permeability hosted the gas hydrate formed with both excess gas and excess water. Effective methane gas permeability was measured in cores with different initial water saturations. The flowrate of the injected methane gas was low and the water was immobile. After complete hydrate formation, the effective gas permeability was measured and evaluated with respect to different hydrate and water saturations. The results showed that the presence of hydrate in the pores highly influenced the effective gas permeability even at constant gas saturations; the effective gas permeability in hydrate-water-gas systems was in some cases reduced with as much as five orders of magnitude compared to the water-gas system. Cores with similar saturations of gas, water and hydrate displayed large variations in effective gas permeability (ranging from µD to mD). The effect of hydrate growth pattern and phase distribution on permeability is discussed, and interpretation of experimental results showed pore-filling hydrate growth in these experiments.

INTRODUCTION
Production of methane gas from natural gas hydrates has experienced growing interest during the last couple of decades due to its vast energy potential [1]. A key factor in all production scenarios is the permeability of the hydrate-filled sediments. Pressure depletion requires sufficient permeability to allow for pressure perturbations to reach within the reservoir and allow for flow of liberated methane gas to production wells. Injection of CO_2 fluid is similarly dependent on adequate permeability in order to maintain flow through the reservoir from injector to producer well. Reservoir simulation models need reliable permeability data to assess the potential of sedimentary hydrate reservoirs as commercial production sites [2]. The goal of permeability studies on hydrate-filled sediments is to

determine whether there is a relationship between hydrate saturation and gas-phase permeability. However, the permeability-saturation correlation is affected by other parameters, most notably the distribution of hydrate in the pore space [3]. The pore-level location of hydrates affects the permeability severely as does also the amount and distribution of free gas and immobile water in addition to hydrates. Immobile water is the water that is left behind after hydrate formation due to capillary trapping or salinity inhibition. Free water is additional water that is left behind because of local unavailability of methane gas. All the free water was immobile during the flow experiments in this study (because of low flowrates of gas), but local formation of additional hydrates may have taken place if injected methane gas came in contact with free water.

Johnson *et al* [4] performed relative permeability tests on unconsolidated sediments retrieved from the Mount Elbert gas hydrate stratigraphic test well in Alaska. Nitrogen gas was used to avoid secondary hydrate formation during injection, and the end-point relative permeability of the gas was measured to be below 0.01 for a core with a hydrate saturation of 0.13 ($S_g \approx 0.25$ and $S_w \approx 0.65$). In fact, the hydrate saturation could not exceed approximately 0.36 in order to provide measurable permeability values, despite the fact that the hydrate interval in Mount Elbert contains twice the amount of hydrates. In comparison, Ahn *et al* [5] found the end-point relative permeability of methane gas to be around 0.1 with a hydrate saturation of 0.15 ($S_g \approx 0.3$ and $S_w \approx 0.55$). The end-point relative permeability in these studies varies with one order of magnitude although the saturations are of comparable size. These results point to the importance of hydrate and fluid distribution, which was not investigated in these experiments. The methodology for creating hydrate was different in the two studies. Ahn *et al* [5] used the excess gas method that is based on pressurizing a water saturated core with gas whereas Johnson *et al* [4] used water to pressurize a core already saturated with gas and water. The excess gas method was previously believed to produce grain-cementing hydrate [6], but other research showed that the method results in pore-filling hydrate growth [3, 7]. Kumar *et al* [8] found the reduction in permeability with increased hydrate saturation to agree with a model based on hydrates coating the mineral surfaces for hydrate saturations below 0.35. For hydrate saturations above 0.35, the agreement was better with a model based on hydrates filling the pore centers. Pore-filling behavior was also observed by Liang *et al* [9] and end-point relative permeability decreased from 0.36 to 0.0036 as hydrate saturations increased from 0.12 to 0.43. One common feature of these previous permeability studies, was that the hydrate saturation was limited to low values. This study investigated the effective gas permeability for intermediate hydrate saturations up to values as high as 0.61. *In situ* hydrate saturations have been quantified to exceed 0.80 in the Mallik gas hydrate field in Canada [10] and tend towards 0.80 in the Daini Atsumi Knoll area of the Eastern Nankai Trough offshore Japan [11]. It is therefore natural to expand hydrate permeability measurements towards higher saturations.

EXPERIMENTAL PROCEDURE

Cylindrical Bentheim sandstone cores (length ≈ 15 cm and diameter ≈ 5 cm) were used as porous medium. They have a fairly constant porosity of 0.22 and an absolute permeability measured before every experiment that ranges between 1.3 and 1.9 D. Every core was saturated to a predefined value with brine containing 3.5 wt% NaCl and then mounted into the rubber sleeve inside the core holder (Figure 1). All pump lines and tubings were purged under vacuum before filling the pumps with methane gas (>99.5%). The core was pressurized to 8.3 MPa from both ends and the overburden pressure was applied by pressurized oil (3 MPa above pore pressure) surrounding the rubber sleeve. Permeability measurements prior to hydrate formation were achieved by injecting methane gas with one pump at the inlet side of the core and producing methane gas with another pump at the outlet side. The volume rate of injection and production was identical and held below 16 mL/min to avoid extraction of water from the core. Differential pressure along the core was recorded with a differential pressure transducer, along with measurements of inlet pressure and core surface temperature. Hydrate formation was initiated by circulation of antifreeze into a cooling jacket that surrounds the core holder and that reduced the temperature to a constant 4°C for all tests. Permeability measurements were repeated when hydrate formation was completed, but at this point the outlet pump was set to hold a constant pressure rather than constant production rate. This was done to avoid artificial under-pressure at the outlet side of the core that could be an issue if the core was completely clogged by hydrates. Flow rates were varied for all permeability measurements and the permeability was calculated for each flow rate by Darcy's law. The reported permeability values are arithmetic averages of the permeability of each flowrate.

RESULTS AND DISCUSSION

Measured permeability values for the range of hydrate saturations in these tests show considerable variability (Table 1). Subscript i refers to initial values, i.e. prior to hydrate formation, and subscript f refers to final values obtained after hydrate formation. Calculation of final saturations are based on PVT-data. The final gas relative permeability shows a strong dependence on the final gas saturation, and a permeability transition zone occurs at a saturation of 0.34-0.38 for these experiments (Figure 2). The effective gas permeability was in the order of µD below this saturation and in the order of mD above this saturation. Experiments 1 and 2 displayed final permeability values in the mD range, but had nearly similar hydrate saturations as experiment 3 and 4 which had final permeability values in the µD range. This demonstrates the importance of all phases found in the pore space and that it is impossible to correlate permeability to hydrate saturation when both excess water and gas reside in the pores. In order to generate basic permeability relationships, it is desirable to remove one of the fluid phases from the experiment, but this is not easy to implement in practice. Complete removal of fluids is impossible due to capillary trapping and even reducing one of the phases to residual saturation may affect the hydrate stability severely and thereby induce melting. Actual attempts to reduce the gas

saturation to residual value by injection of precooled water have shown to induce hydrate dissociation [12]. Water production was not monitored continuously during the permeability measurements in this study but visual inspection of the outlet pump cylinder after each experiment showed no sign of water. However, there was a small increase in permeability with increased flowrate for the cores with low final gas saturation (<0.34). Some of these cores did also experience a small decline in differential pressure at constant flowrate. Limited water production may thus have taken place in these experiments and the final permeability will then be an average over a slightly varying gas saturation.

Pore-space distribution of phases was not explicitly investigated in these experiments. The location of fluids within the porous media affects the permeability significantly and utilization of any kind of imaging device would improve the understanding of flow behavior. Some comments can nevertheless be given regarding hydrate growth. As previously mentioned, permeability values dropped to µD-scale when the gas saturation was lower than 0.34-0.38 after hydrate formation. In experiment 8, the permeability prior to hydrate formation was measured to be 57 mD for a gas saturation of only 0.27. The final permeability was not just limited by the low gas saturation for experiment 3-8, but the presence of hydrates in the pores seemed to decrease the permeability further. The observation that the permeability was lower for a gas-water-hydrate system compared with a gas-water system for approximately equal gas saturations, indicates that the hydrate growth occurred in the pore bodies. The configuration of fluids prior to hydrate formation is believed to consist of gas occupying the interior of the biggest pores due to the strong water-wet nature of Bentheim sandstone. Initial hydrate growth in the pore throats would have notably reduced the connectivity of the gas phase from pore to pore and is not likely because of relatively high permeability for hydrate saturations of almost 0.50 (experiment 1 and 2). Pore-coating hydrate growth in the large pores would have had little effect on the permeability-reduction even for intermediate hydrate saturations as the gas could flow in the middle of the pores, and is also unlikely (e.g. experiment 6 and 7). The observed permeability can best be explained by pore-filling hydrate growth. Hydrate occupying the center of large pores obstructed the flow significantly when the hydrate saturation reached intermediate/high values, and the gas permeability was lower when hydrates were present for similar gas saturations. However, a situation described by Kumar *et al* [8], where the hydrate growth was pore-coating for low saturations and pore-filling for high saturations, is possible.

CONCLUSIONS
Effective gas permeability for hydrate-filled sandstone cores was measured in a series of experiments. The methane hydrate saturation varied between 0.37-0.61 and immobile excess water was present during permeability measurements. The effective gas permeability decreased from mD-scale to µD-scale when the gas saturation dropped below 0.34-0.38 independent of the hydrate saturation. However, comparison of different experiments showed that the presence of hydrate decreased the permeability even though

the gas saturation was constant. This indicated pore-filling hydrate growth for the experiments conducted in this study.

REFERENCES

1. Kvenvolden, K.A., "Origins of Methane in the Earth Methane hydrate — A major reservoir of carbon in the shallow geosphere?", *Chemical Geology*, (1988) **71**, 1, p. 41-51.
2. Moridis, G.J., T.S. Collett, R. Boswell, M. Kurihara, M.T. Reagan, C. Koh and E.D. Sloan, "Toward Production From Gas Hydrates: Current Status, Assessment of Resources, and Simulation-Based Evaluation of Technology and Potential", *SPE Reservoir Evaluation & Engineering*, (2009) **12**, 5, p. 745-771.
3. Kleinberg, R.L., C. Flaum, D.D. Griffin, P.G. Brewer, G.E. Malby, E.T. Peltzer and J.P. Yesinowski, "Deep sea NMR: Methane hydrate growth habit in porous media and its relationship to hydraulic permeability, deposit accumulation, and submarine slope stability", *JOURNAL OF GEOPHYSICAL RESEARCH*, (2003) **108**, B10, p. 1-17.
4. Johnson, A., S. Patil and A. Dandekar, "Experimental investigation of gas-water relative permeability for gas-hydrate-bearing sediments from the Mount Elbert Gas Hydrate Stratigraphic Test Well, Alaska North Slope", *Marine and Petroleum Geology*, (2011) **28**, 2, p. 419-426.
5. Ahn, T., J. Lee, D.G. Huh and J.M. Kang, "Experimental Study on Two-phase Flow in Artificial Hydrate-bearing Sediments", *Geosystem Engineering*, (2005) **8**, 4, p. 101-104.
6. Waite, W.F., W.J. Winters and D.H. Mason, "Methane hydrate formation in partially water-saturated Ottawa sand", *American Mineralogist*, (2004) **89**, 8-9, p. 1202-1207.
7. Kneafsey, T.J., Y. Seol, A. Gupta and L. Tomutsa, "Permeability of Laboratory-Formed Methane-Hydrate-Bearing Sand: Measurements and Observations Using X-Ray Computed Tomography", *SPE Journal*, (2011) **16**, 1, p. 78-94.
8. Kumar, A., B. Maini, P.R. Bishnoi, M. Clarke, O. Zatsepina and S. Srinivasan, "Experimental determination of permeability in the presence of hydrates and its effect on the dissociation characteristics of gas hydrates in porous media", *Journal of Petroleum Science and Engineering*, (2010) **70**, 1–2, p. 114-122.
9. Liang, H., Y. Song, Y. Chen and Y. Liu, "The Measurement of Permeability of Porous Media with Methane Hydrate", *Petroleum Science and Technology*, (2011) **29**, 1, p. 79-87.
10. Dallimore, S.R., T.S. Collett, T. Uchida, M. Weber, H. Takahashi and T. Mroz, "Overview of Gas Hydrate Research at the Mallik Field in the Mackenzie Delta, Northwest Territories, Canada". Presentation, (2004).
11. Yamamoto, K., Y. Terao, T. Fujii, T. Ikawa, M. Seki, M. Matsuzawa and T. Kanno, "Operational overview of the first offshore production test of methane hydrates in the Eastern Nankai Trough", in *Offshore Technology Conference*, (2014), Houston, Texas, USA.

12. Li, B., X.S. Li, G. Li, J.L. Jia and J.C. Feng, "Measurements of Water Permeability in Unconsolidated Porous Media with Methane Hydrate Formation", *Energies*, (2013) **6**, 7, p. 3622-3636.
13. Hågenvik, C., "CO2 Injection in Hydrate Bearing Sandstone with Excess Water". MSc., Department of Physics and Technology, University of Bergen, Norway, (2013).
14. Ersland, G., J. Husebø, A. Graue, B. Kvamme, B. Baldwin, J.J. Howard and J. Stevens, "Measurements of Gas Permeability and Non-Darcy Flow in Gas-Water Hydrate Systems", in *Proceedings of the 6th International Conference on Gas Hydrates*, (2008), Vancouver, Canada.

Table 1. List of all experiments with related saturations and permeability values. Margins of error reflect equipment uncertainties.

Experiment ID	K_{abs} [D]	S_{wi} ±0.01	S_{gi} ±0.01	K_i [D]	S_{wf} ±0.02	$S_{hydrate}$ ±0.02	S_{gf} ±0.02	K_f [µD]	K_f [mD]	k_r
1	1.7 ±0.2	0.46	0.54	0.20 ±0.02	0.10	0.46	0.44		32 ±3	0.019 ±0.003
2	1.9 ±0.6	0.53	0.47	0.4 ±0.1	0.17	0.47	0.37		2.3 ±0.4	0.0012 ±0.0004
3	1.6*	0.54	0.46	0.14 ±0.02	0.19	0.45	0.37	2.52 ±0.02		1.6E-06 ±0.2E-06
4	1.6*	0.54	0.46	0.09 ±0.02	0.17	0.47	0.36	6.1 ±0.1		3.8E-06 ±0.5E-06
5	1.6*	0.54	0.46	0.088 ±0.008	0.14	0.51	0.35		0.20 ±0.02	0.00013 ±0.00002
6	1.9 ±0.6	0.64	0.36	0.15 ±0.02	0.16	0.61	0.23	0.851 ±0.005		4E-07 ±1E-07
7	1.3 ±0.1	0.64	0.36	0.18 ±0.02	0.23	0.53	0.24	1.277 ±0.005		9.9E-07 ±0.8E-07
8	1.8 ±0.2	0.73	0.27	0.057 ±0.008	0.45	0.37	0.19	1.25 ±0.01		7.1E-07 ±0.8E-07

*Absolute permeability was not measured. The given value is the midpoint of the other permeability values.
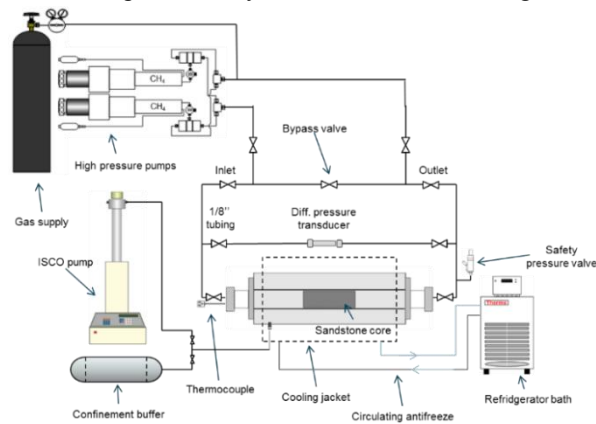

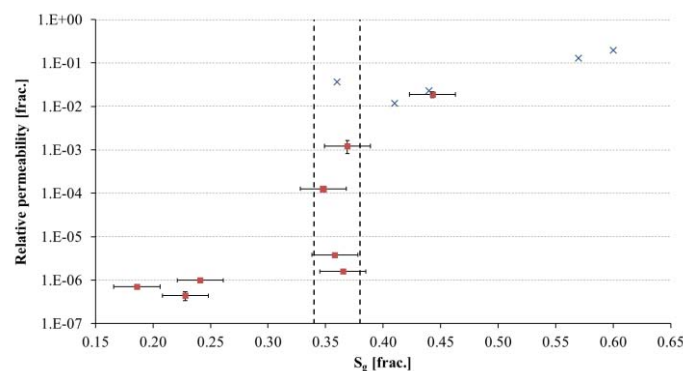**Figure 1.** Experimental setup. Modified from Hågenvik [13].

Figure 2. Gas relative permeability after hydrate formation. The data points denoted as crosses (blue) are permeability values obtained by Ersland *et al* [14]. A transition zone between S_g = 0.34-0.38 is indicated by vertical dotted lines. Margins of error reflect equipment uncertainties.